AIP | Journal of Applied Physics

Transport properties of polypyrrole–ferric oxide conducting nanocomposites

R. Gangopadhyay, A. De, and S. Das

Citation: J. Appl. Phys. **87**, 2363 (2000); doi: 10.1063/1.372188
View online: http://dx.doi.org/10.1063/1.372188
View Table of Contents: http://jap.aip.org/resource/1/JAPIAU/v87/i5
Published by the American Institute of Physics.

Transport properties of polypyrrole–ferric oxide conducting nanocomposites

R. Gangopadhyay and A. De[a)]
Nuclear Chemistry Division, Saha Institute of Nuclear Physics, 1/AF Bidhannagar, Calcutta 700 064, India

S. Das
Solid State and Molecular Physics Division, Saha Institute of Nuclear Physics, 1/AF Bidhannagar, Calcutta 700 064, India

(Received 22 June 1999; accepted for publication 22 November 1999)

Conducting nanocomposite samples were prepared combining colloidal ferric oxide particles with conducting polypyrrole. Three composite samples (prepared keeping colloidal content fixed and varying the content of the conducting polypyrrole) and the pure polymer were used in the present investigation. Temperature dependent dc and ac conductivity and thermoelectric power for the samples have been measured. The dc conductivity results were analyzed by Mott's variable range hopping mechanism. The variation of ac conductivity with the frequency shows very little change in total conductivity up to a critical frequency, followed by a sudden jump with discontinuity and then increases monotonically following a power law. The frequency exponent decreases with temperature as predicted by the correlated barrier hopping theory. Above 50 K the ac component of the conductivity increases almost linearly as predicted by the quantum mechanical tunneling model. It is found that all the features of ac conductivity cannot be reconciled into an existing single theory. The thermoelectric power is positive, low, and varies linearly with temperature, indicating a metallic character and the presence of polarons and/or bipolarons as the cationic charge carriers in the composites. The overall nature of the $S(T)$ curves suggests that in addition to a contribution from hopping a linear metallike component is also active for the thermopower. © *2000 American Institute of Physics.* [S0021-8979(00)04005-6]

I. INTRODUCTION

Research activity in the field of polymer science has taken a new lead after the advent of inherently conducting polymers (ICPs). Owing to their very interesting and important electrical and electronic properties, these materials have raised a great deal of fundamental scientific interest as well as possibilities of novel applications over the past 2 decades. However, the inherent difficulties with these materials, namely their lack of processability and poor mechanical properties, have led the bulk of investigations toward some suitable modifications of the existing polymers, so that their applicability can be improved. This way of synthesizing novel polymeric materials with unique electrical properties and good processability have given birth to a large number of blends and composites[1–4] in which the conducting polymers are mixed up with some processable insulating polymers in different techniques to successfully combine the properties of both components. In parallel with the synthesis of the conventional composites, over the last few years, a large number of articles have been published reporting on the effective combination of some ultrafine particles of different metals, metal oxides, and some structured materials with the conducting polymers, resulting in the formation of composite nanoparticles or nanomaterials, specifically termed polymeric nanocomposites. Inorganic particles namely SiO_2,[5–7] SnO_2,[8,9] $BaSO_4$,[10] TiO_2,[11] ZrO_2,[12] colloidal gold,[13] etc. and structured materials namely Montmorrilonite,[14] Zeolites,[15] microporous membranes of polycarbonate,[16] etc. have so far been successfully combined with polyaniline (PAn) and polypyrrole (PPy) in some easy chemical and electrochemical processes to give rise to a variety of such nanocomposites, morphology, and different physical properties of which have been widely studied. Most of these materials can bring the intractable conducting polymer in a stable colloidal form. dc conductivity and some other physical properties have also been improved in some reports.[12]

Apart from the knowledge on the physical and material properties, a thorough understanding of the charge transport mechanism of the ICPs and their composites is important for successful fabrication of sophisticated devices. But no single unanimous model is so far available that can properly describe the prevailing conduction processes occurring through the presence of nonlinear excitations like solitons, polarons, and bipolarons in these solids. Generally the lattices of organic systems like PAn, PPy, etc., are very soft and the electronic state can easily be altered, resulting in significant structural and electronic rearrangements. The removal or acceptance of electrons results in *p*-type or *n*-type doping, which distorts the polymer lattice around the injected charge. The carriers generated in this process are known to be self-trapped by the conjugated polymeric chains in the form of polarons or bipolarons, which are placed in the localized states due to random electric fields near the Fermi level. If

[a)]Author to whom correspondence should be addressed; electronic mail: amitde@nue.saha.ernet.in.

the polarons and bipolarons are mobile with long enough lifetime, then they may act as charge carriers. Conduction may occur by the thermal hopping of electrons between quantized localized states at the cost of activation energy. The quasione-dimensional morphology produced by the covalent bonding along the polymer chain and also the weak bonding among them helps in the charge delocalization of the system. Up to the intermediate doping levels, the stable ground states are confirmed to be polarons, whereas at higher doping levels both polarons and bipolarons may be created.

Recently we have reported the synthesis and characterizations of a series of conducting nanocomposites in which colloidal ferric oxide particles have been combined with different amount of PPy.[17] In this system the PPy:Fe_2O_3 ratio (w/w) is kept above the percolation threshold and the Fe_2O_3 particles are entrapped or encapsulated in PPy matrix, resulting in some significant improvement of the physical properties of pure polymer (PPy). However the detailed studies on the nature of carriers governing the electrical transport were awaited there. Earlier workers have studied the transport properties in conventional composites and blends like PMMA-PAn,[18] PVA-PPy,[19] PS-PAn,[20] etc. following temperature dependent dc electrical conductivity and thermoelectric power (TEP) measurements. Most of them recognized the mechanism of conduction in such systems as hopping of carriers between localized states. Mott's VRH theory is applicable in general, while Jousseame *et al.* have applied the Zuppiroli model to the PVA-PPy[19] system. Temperature dependent data of PMMA-PAn composite[21] have revealed somewhat metallic behavior of the system over the temperature range 10–300 K. Such studies so far are not frequently available in nanocomposite systems. In order to get a complete and coherent picture of the conduction mechanism in the present PPy–Fe_2O_3 system we have studied these composites by temperature dependent dc and ac conductivity and thermoelectric power measurements. ac conductivity measurement has an added advantage of separating interchain charge transfer (low frequency region) from intrachain electronic conduction (high frequency region), which is scarcely available in the field of conducting polymer composites/nanocomposites, especially with the heavily doped systems. Most of the previous results relate mainly to the pure conducting polymers (PPy and PAn) in lightly doped states. Therefore the present studies and the corresponding results are expected to reveal the underlying mechanism of electrical transport in the PPy–Fe_2O_3 nanocomposite system and to provide an idea about the nature of the carriers in these materials. It is worth mentioning here that all the samples studied are heavily doped, prepared above percolation threshold and ac measurements are carried out in the high frequency regime.

II. EXPERIMENT

Preparation of samples is already reported in one of our recent publications.[17] However, the same is briefly described here. Ferric oxide (Fe_2O_3) colloid having particles of 25–50 nm was synthesized using a standard technique. In the presence of a fixed volume (50 ml) of the colloid, different volume of pyrrole was polymerized with ferric chloride ($FeCl_3$) initiator keeping the pyrrole: $FeCl_3$ mole ratio at 1:2.5. Black solid precipitate formed was filtered, washed, and vacuum dried at 50 °C.

A. dc conductivity

dc electrical conductivity was measured from pressed pellets of the samples over the temperature range 25–300 K, following standard four probe technique. Samples were mounted on a cryotip and were placed inside Oxford (model 22) closed cycle helium refrigerator. A constant current (dc) was passed through the samples from a Lake Shore cryotonics (model 120) constant current source and voltage drop across the samples was measured with a Keithley (model 182) nanovoltmeter. Lake Shore cryotonics (model DTC 500 A) temperature controller was used for controlling the temperature of the system.

B. ac conductivity

ac conductivities of the samples were measured over the temperature range 14–300 K using the two probe method. Samples were placed in an APD cryotip attached with a Lake Shore Autotuning temperature controller. The admittance and phase angle values were measured with a precision RCL Bridge (QuadTech 7600) over a frequency range 500 kHz–2 MHz. The real part of the conductivity was calculated from the admittance and the phase angle expressed in radians.

C. Thermoelectric power

TEP of the samples was measured using the differential technique over the temperature range 77–300 K. A temperature gradient ΔT across the samples using two heaters and voltage developed ΔE between the hot and the cold ends of the thermocouple formed by the samples and Cu wires were measured. Pressed pellets of samples were mounted by pressure contact between the copper plates and the whole system was placed in a glass Dewer, attached with a temperature controller (Lake Shore cryotonic, DRC-93CA), and interfaced with a computer which records the TEP values as a function of temperature.

III. RESULTS AND DISCUSSION

A. dc conductivity

Figure 1 presents Ln σ of the samples as a function of reciprocal temperature. The nonlinearity of this curve indicates temperature dependent activation energy and suggests that the band conduction model is not sufficient to explain the conduction mechanism in these composites. Semiconductor theory shows that the temperature dependent energy gap cannot explain the experimental results since it should be more than linear in order to account for the temperature dependent activation energy.[22] Mott[23,24] has investigated a conduction model considering the conduction process in terms of phonon assisted hopping of small polarons between localized states. The dc conductivity in this model is given by

$$\sigma_{dc} = \sigma_0 \exp(-W_g/k_B T), \quad (1)$$

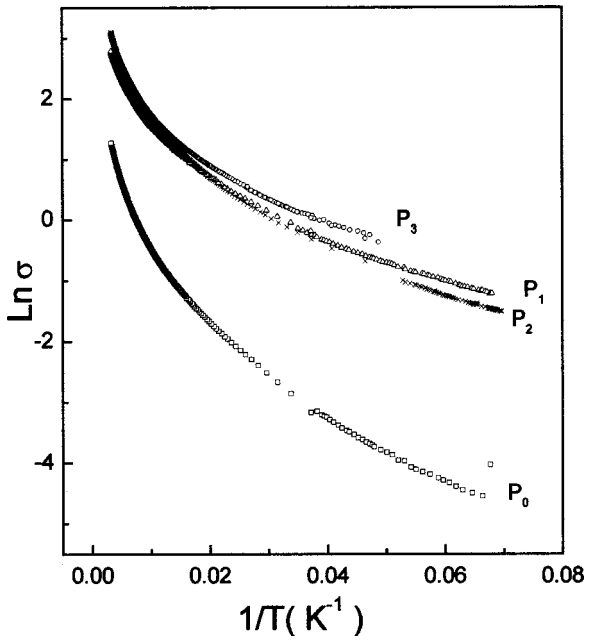

FIG. 1. The natural logarithmic dc conductivity ($\ln \sigma$) as a function of temperature for all the samples studied.

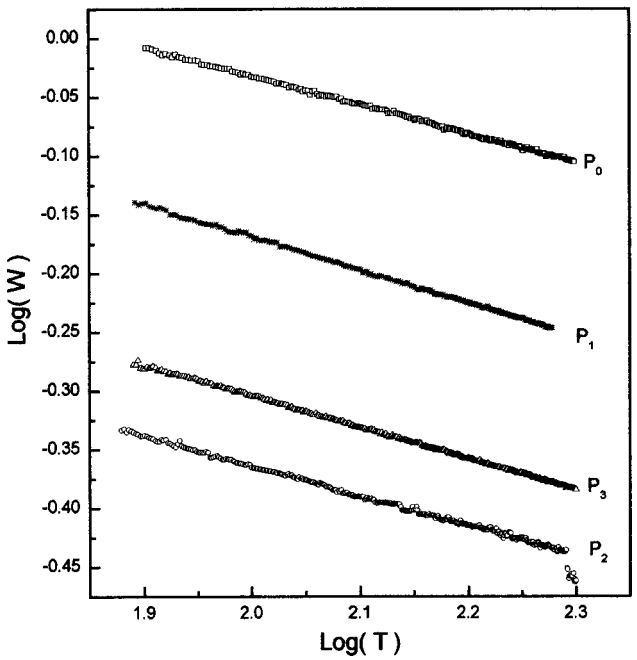

FIG. 2. A log–log plot of $W(=Td[\ln \sigma]/dT)$ against T for the four samples.

where σ_0 is the preexponential constant, k_B is the Boltzmann constant, and W_g is the activation energy for dc conduction. This activation energy consists of the polaron hopping energy W_H and an energy difference W_D between localized states due to disorder. Austin and Mott[25] have shown that

$$W_g = W_H + W_D/2 \quad \text{for } T > \theta_D/2,$$
$$= W_D \quad \text{for } T < \theta_D/4,$$

where θ_D, defined by $h\nu_0 = k_B\theta_D$ is the characteristic Debye temperature and ν_0 is the phonon frequency. Now one can consider the lowest temperature activation energy as a measure of the disorder energy W_D and calculate the value of ν_0 considering the limiting value $h\nu_0 \cong W_D/2$. Calculated values of ν_0 and θ_D for four samples are shown in the Table I. Parameters derived from this analysis are unacceptably low and not very reasonable. In the temperature regime where the electron–phonon interaction is strong enough, the static disorder energy plays a dominant role in the conduction process. Mott has suggested a variable range hopping mechanism of the polaron and in this model the temperature dependence of the electrical conductivity due to polaron hopping is described by the relation

TABLE I. Parameters obtained by fitting the dc conductivity data of the four samples to the Mott–Austin model.

Sample	Activation energy at high temperature (eV)	Activation energy at low temperature (W_D) (eV)	$\nu_0 \cong W_D/2h$ s^{-1}	$\theta_D = h\nu_0/k = W_D/2$ K
P_0	0.038	0.005	3.8×10^{12}	29
P_1	0.026	0.003	2.24×10^{12}	17.12
P_2	0.027	0.0033	2.51×10^{12}	19.15
P_3	0.0298	0.003	2.13×10^{12}	16.25

$$\sigma = \sigma_0 \exp[-(T_0/T)^{1/n}], \tag{2}$$

where the exponent n is 4 for three dimensional and 3 for two dimensional hopping.

The characteristic Mott temperature T_0 and the preexponential factor σ_0 are expressed as

$$T_0 = \lambda\alpha^3/k_B N(E_F), \tag{3}$$

and

$$\sigma_0 = e^2R^2\nu_0 N(E_F), \tag{4}$$

where λ is a dimensionless constant ($\sim$18.1),[26–29] k_B is the Boltzmann constant, α describes the spatial extent of localized wave function, $N(E_F)$ is the density of states at the Fermi level, and ν_0 is the phonon frequency. T_0 can be considered as an effective energy barrier between localized states and measures the extent of disorder in the disordered region. A larger value of T_0 implies greater disorder. The hopping distance R can be given by

$$R = \{9/[8\pi\alpha k_B TN(E_F)]\}^{1/4}. \tag{5}$$

In order to explicitly determine the VRH exponent n, we define the reduced activation energy W as

$$W(T) = Td[\ln \sigma]/dT. \tag{6}$$

Combining Eqs. (2) and (6) we get

$$\log_{10} W(T) = A - n \log_{10} T, \tag{7}$$

where $A = n \log T_0 + \log n$. The slope of the plot of $\log_{10} W$ against $\log_{10} T$ gives the value of n. In Fig. 2 we have plotted the $W(T)$ curve for the four samples. The value of n obtained from the fitting of the $W(T)$ curves are 0.24 for P_0, 0.26 for P_1, 0.25 for P_2, and 0.24 for P_3. So this plot indicates that the three dimensional VRH mechanism plays an important role in the conduction process in these composites.

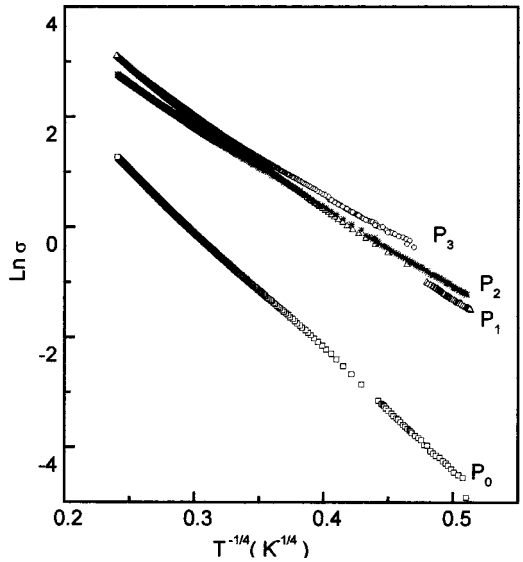

FIG. 3. Variation of Ln σ as a function of $T^{1/4}$ for different samples (to avoid clumsiness theoretical curves are not shown).

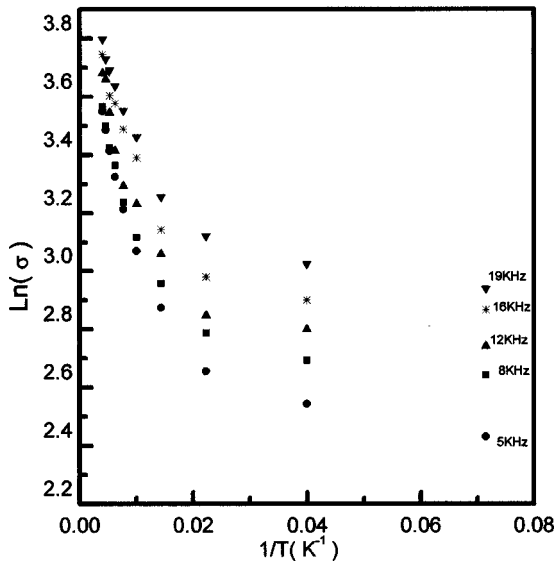

FIG. 4. The measured total conductivity (Ln σ) of the composite P_2 as a function of reciprocal temperature for five different frequencies.

Ln $\sigma(T)$ has been plotted against $T^{1/4}$ in Fig. 3. The linear behavior of the curves show that the value of n used here is consistent with that obtained from the $\log_{10} W$ against $\log_{10} T$ curves. From the calculations of the energetics of polaron and bipolaron formation on pyrrole chains Bredas *et al.*[30] have shown that the polaron and bipolaron length extends over to about four pyrrole rings. Moreover, Singh *et al.*[31] found the polaron radius to be equal to 1.82 A^0. To analyze the data in light of Mott's VRH theory we have assumed that the localization length (α^{-1}) is 10 A^0 (extending up to four pyrrole rings) in one case and 1.5 A^0 (close to polaron radius) in another. Table II presents the different parameters of the four samples obtained by fitting with Mott's VRH theory.

For relatively low conducting composites, $N(\epsilon_F)$ values are low and the charge transport follows the hopping mechanism. But for relatively high conducting composites, $N(\epsilon_F)$ has higher value and the mobility of polarons and bipolarons may play a significant role in increasing the total conductivity. According to the Mott's VRH theory the parameter T_0 is inversely proportional to the localization length of the charge carriers. Therefore a large value of T_0 implies strong localization of the charge carriers which result in increasing the resistance at low temperatures, whereas a small value of T_0 implies weak localization.

B. ac conductivity

Figure 4 represents the total conductivity σ_{tot} of the sample P_2 plotted as a function of reciprocal temperature at different frequencies. The curve does not show any linear behavior throughout the temperature range studied, i.e., no activated type of behavior is observed. Other samples with different compositions also behave similarly. It is observed that the measured conductivities at all frequencies coincide with σ_{dc} at high temperatures. At low temperatures, the temperature dependence of σ_{tot} is much less than σ_{dc} but increases at higher temperatures.

TABLE II. Variable range hopping parameters for bare polypyrrole and composites.

Sample specification	Colloid content (ml)	Volume of pyrrole (ml)	Characteristic temperature, T_0	Preexponential factor (σ_0)	Density of states $N(E_F)$ ($eV^{-1}\,cm^{-3}$)	Hopping distance, R_{300} (at 300 K)	Hopping attempt frequency $\times 10^{-13}$
			with $\alpha^{-1}=10$ (Å)				
P_0	0.0	···	298250	979	7.04×10^{20}	21.06×10^{-8}	13.59
P_1	50.0	0.35	73102	829	2.87×10^{21}	14.82×10^{-8}	5.70
P_2	50.0	0.30	92640	1420	2.27×10^{21}	15.72×10^{-8}	10.99
P_3	50.0	0.25	159456	2696	1.32×10^{21}	18.01×10^{-8}	27.37
			with $\alpha^{-1}=1.5$ (Å)				
P_0			298250	979	20.87×10^{22}	3.16×10^{-8}	2.04
P_1	50.0	0.35	73102	829	85.14×10^{22}	2.22×10^{-8}	0.854
P_2	50.0	0.30	92640	1420	67.18×10^{22}	2.36×10^{-8}	1.65
P_3	50.0	0.25	159456	2696	39.03×10^{22}	2.70×10^{-8}	4.103

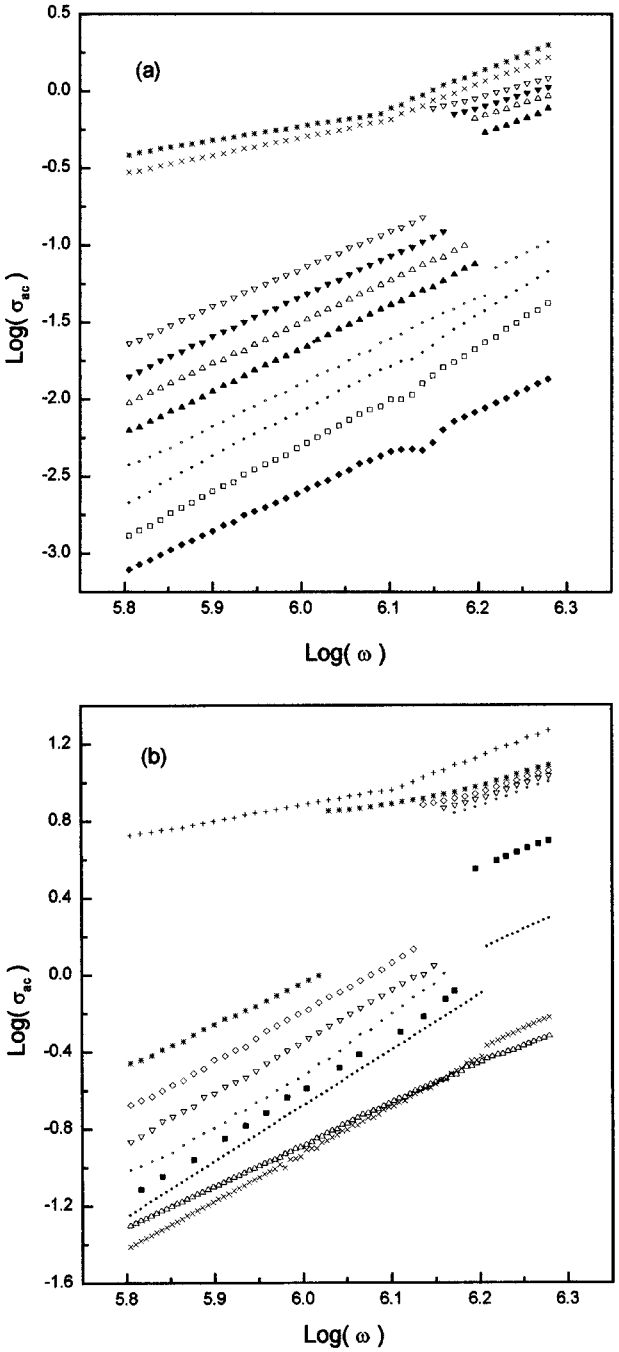

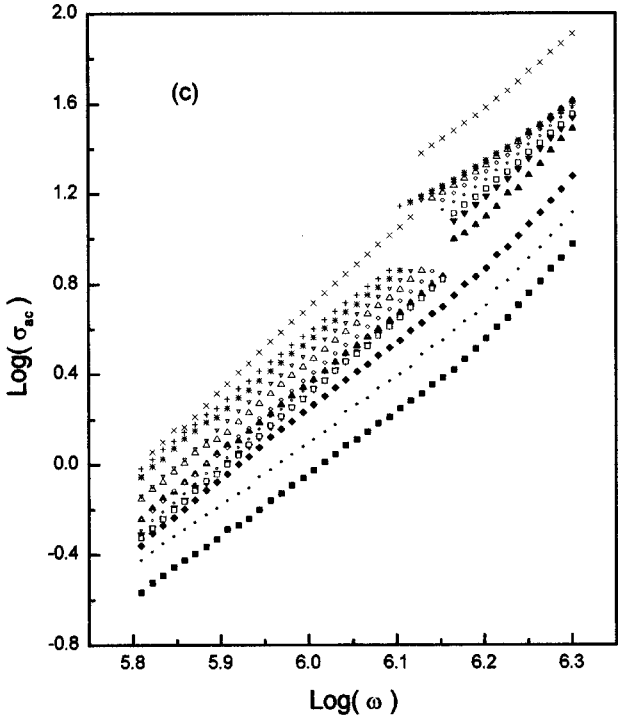

FIG. 5. (a) Frequency dependence of the ac conductivity for the bare polymer P_0 at several fixed temperatures (log–log plot). (From top to bottom: $T=250$, 225, 165, 145, 125, 105, 85, 65, 35, 14 K). (b) Log σ_{ac} vs Log ω curve for the composite P_2. (From top to bottom: $T=250$, 220, 190, 160, 130, 100, 70, 45, 14 K). (c) Variations in logarithmic ac conductivity with frequency for the composite P_3. (From top to bottom: $T=300$, 275, 250, 200, 175, 105, 150, 125, 100, 75, 55, 35, 13 K).

A common feature of amorphous semiconductors and disordered systems is that the frequency dependent conductivity obeys a power law[32–34] given by

$$\sigma(\omega)=A\omega^{s}, \tag{8}$$

where A is a temperature dependent constant and the frequency exponent $s\leqslant 1$. The origin of this almost universal behavior remains controversial and it is often thought that it arises from the relaxation processes due to hopping or tunneling of electrons or atoms between equilibrium sites.

When ac and dc conductivity appears from completely separate and different processes, the total conductivity can be written as

$$\sigma_{tot}=\sigma_{dc}+\sigma(\omega). \tag{9}$$

If dc and ac conduction originates from the same mechanism, then the dc conductivity equalizes the ac conductivity in the limit $\omega\rightarrow 0$.

The variation of ac conductivity as a function of frequency at different temperatures is shown in Figs. 5(a), and 5(b) and 5(c) for the samples P_0, P_2, and P_3, respectively (log–log plot). It is seen from the figure that the logarithmic ac conductivity varies linearly with the change of logarithmic frequency. At a critical frequency a discontinuity appears and then the conductivity increases monotonically. The characteristic frequency at which the discontinuity appears, decreases with the increase of temperature and in the frequency range where $\sigma(\omega)\gg\sigma_{dc},\sigma(\omega)$ attains a power law behavior. Figures 5(a), 5(b), and 5(c) show that the ac con-

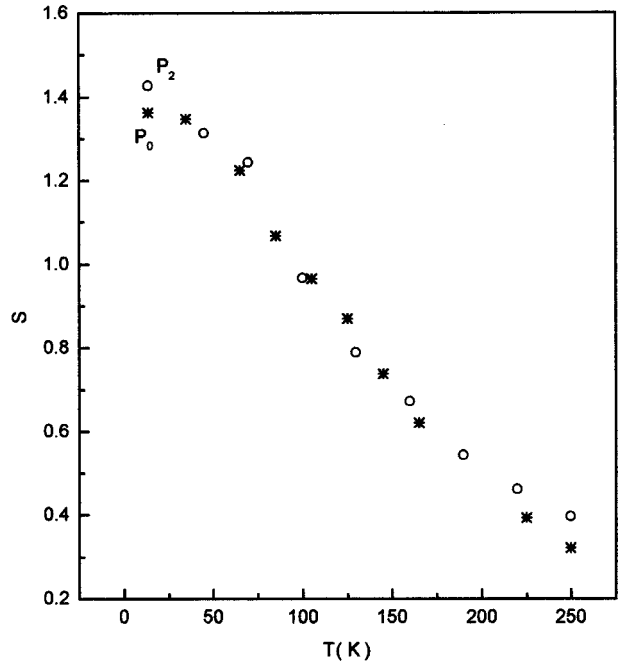

FIG. 6. Temperature dependence of the frequency exponent **s** for the samples P_0 and P_2.

ductivity plays a significant and dominant role at high frequencies and low temperatures. The dc conductivity can be determined from the plateau region of the σ_{tot} vs ω curve. The σ_{dc} values estimated from σ_{tot} agree well with the value obtained from the dc conductivity measurement. The ac conductivity $\sigma(\omega)$ was calculated by subtracting the dc contribution from σ_{tot} and calculated $\sigma(\omega)$ was fitted by the least square method using Eq. (8) in the frequency range from the critical frequency to the highest frequency measured. The variation of the frequency exponent **s** with the temperature is presented in Fig. 6 for the samples P_0 and P_2. From the figure it is observed that **s** decreases with the increase of temperature. For P_0 and P_2, **s** assumes a value greater than 1 in the temperature domain below 90 K and for the sample P_3 it lies above 1 in the whole temperature range. It should be mentioned here that for P_3 the frequency exponent is found to depend on the frequency, which becomes significant at high temperatures [Fig. 5(c)]. Although there is a slight frequency dependence of **s** for P_2, no such behavior was found in the case of P_0 [Figs. 5(a) and 5(b)]. Any deviation from the value of **s** from unity discloses information on the particular type of loss mechanism involved. The discontinuity observed in Figs. 5(a), 5(b), and 5(c) is both frequency and temperature dependent. The frequency where the discontinuity appeared, decreases as the temperature increases. The ac conductivity results[35–37] published so far for polypyrrole did not show any discontinuity. It is not possible to compare our results with those because the measurements were performed within the frequency range less than 1 MHz for lightly doped polypyrrole. But here the discontinuity appeared at frequencies greater than 1 MHz. In Ref. 38 the ac conductivity of polypyrrole–poly(ethylene) oxide composite showed discontinuity in the frequency regime higher than 1 MHz for heavily doped systems. A sudden rise in the conductivity value in our results at the critical frequency indicates that some form of polarization becomes active at the critical frequency. In order to understand the origin of this phenomenon a more detailed study is necessary.

Many models have been proposed to explain the dispersion of ac conductivity in inhomogeneous media but no unanimous interpretation of the experimental results has been reached. In each of the models, the relaxation processes involved in the ac responses are assumed to be described by the pair approximation introduced by Pollock and Geballe.[39] Here the charge transfer occurs in pairs and the total response results from the sum of the individual responses of the pair of sites randomly distributed throughout the material. It is also assumed that the clusters of more than two sites do not contribute to the ac conductivity. In this model averages are carried out over the appropriate distribution of relaxation time parameter of a Debye-type dielectric response function and the relaxation processes includes an activation energy appearing due to the disordered structure of the material. Let us now summarize the predictions of the different models relating to the temperature dependence of $\sigma(\omega)$ and **s** so that they can be compared with the experimental findings on the present system.

1. Electronic tunneling

If the dielectric loss originates from the electronic relaxation, then the charge transfer may occur by the quantum mechanical tunneling (QMT) through a barrier. In the QMT model[40–43] the real part of the ac conductivity at a particular frequency ω can be expressed as

$$\sigma(\omega)=(\pi^4/24)(e^2kT/\alpha)N^2(E_F)\omega R_\omega^4, \tag{10}$$

where the quantities have their usual meaning and the characteristic tunneling distance

$$R_\omega=(2\alpha)^{-1}\ln(1/\omega\tau_0). \tag{11}$$

The frequency exponent is defined by

$$\mathbf{s}=d\ln\sigma(\omega)/d\ln\omega, \tag{12}$$

and here

$$\mathbf{s}=1-4\ln(1/\omega\tau_0). \tag{13}$$

For typical values of $\omega=10^4\ \text{s}^{-1}$ and $\tau_0=10^{13}$ s, $\mathbf{s}=0.8$ and is less than one. From this model **s** is predicted to be temperature independent but frequency dependent, decreasing with the increase of frequency.

2. Small polaron tunneling

If the carriers become nonoverlapping small polarons, **s** becomes temperature dependent in the framework of the QMT model. The ac conductivity follow the same expression as Eq. (10) but the tunneling distance takes the form

$$R_\omega=(2\alpha)^{-1}[\ln(1/\omega\tau_0)-W_H/kT]. \tag{14}$$

The frequency exponent **s** can be written as

$$\mathbf{s}=1-4/[\ln(1/\omega\tau_0)-W_H/kT], \tag{15}$$

i.e., **s** is temperature dependent and increases as T increases.

3. Large polaron tunneling[43,44]

Long[43] has proposed a polaron tunneling model where the polaron distortion cloud overlaps appreciably, i.e., the potential wells of neighboring sites overlap reducing the polaron hopping energy so that

$$W_H = W_{H0}(1 - r_0/R), \tag{16}$$

where r_0 is the polaron radius and R is a random variable.

This overlapping large polaron model predicts that **s** should be both temperature and frequency dependent. With the increase of temperature **s** falls from unity and approaches the value 0.8 as predicted by the QMT model for large values of $r_0'(\equiv 2\alpha r_0)$. For small values of r_0',**s** shows a minimum at a particular temperature and then increases with the rise of temperature. For large values of r_0',$\sigma(\omega)$ decreases with the rise of temperature.

4. Correlated barrier hopping (CBH) of electrons

In the atomic hopping model the relaxation variable is assumed to be independent of inter site separation. Pike[45] has removed this restriction and proposed a model of electron transfer by thermal activation over the barrier between two adjacent sites. The Coulomb potential wells associated with the sites overlap and lower the effective barrier from W_M to W, which in the case of single electron transition is given by

$$W = W_M - e/\pi\epsilon\epsilon_0 R, \tag{17}$$

where W_M is the value of infinite site separation and ϵ and ϵ_0 are the dielectric constants of the materials and the free space, respectively.

In this CBH model[34,45,46] the ac conductivity was calculated in the narrow band limit to be

$$\sigma(\omega) = (\pi^3/24)N^2\epsilon\epsilon_0\omega R_\omega^6, \tag{18}$$

where N is the concentration of the pair sites.

The hopping distance R_ω is given by

$$R_\omega = e^2/\pi\epsilon\epsilon_0[W_M - kT\ln(1/\omega\tau_0)]. \tag{19}$$

The frequency exponent **s** is expressed as

$$\mathbf{s} = 1 - 6kT/[W_M - kT\ln(1/\omega\tau_0)]. \tag{20}$$

Therefore, **s** is both temperature and frequency dependent. **s** is predicted to decrease with increasing temperature and at low temperature (i.e., large W_M/kT) **s** decreases almost linearly from unity (the value at $T=0$). At higher temperatures, i.e., for small values of W_M/kT,**s** increases with increasing frequency and for large values of W_M/kT, **s** is close to unity and effectively independent of frequency.

The experimental observation about the composites studied conflicts with the predictions of the electronic QMT model, which predicts a temperature independent value of **s** ($=0.81$ for typical values of ω and ν_0). Again the QMT model of the nonoverlapping small polaron predicts a temperature dependence of s, which increases with the increase in temperature in contradiction to our experimental observation, which shows that the frequency exponent **s** decreases with increasing temperature. According to the QMT model **s** should decrease with the increase of frequency, but no such variation is observed for the present system in the investigated frequency range. The large polaron tunneling is also not a suitable relaxation mechanism because this model predicts a minimum in the temperature variation of **s**. This is not observed in the case of the present composite system. The value of **s** behaves as predicted by the CBH model. Such behavior of **s** was found in the study of ac conductivity of V_2O_5–GeO_2 glasses[47] and PbO–Fe_2O_3 glasses.[48] In sharp contrast to all the theories described above, the value of **s** for the composite P_3 is always greater than unity. According to the QMT model the temperature dependence of the ac conductivity follows $\sigma(\omega)\propto T^n$ with $n=1$. Figures 7(a) and 7(b) depict the temperature dependence of the ac conductivity of the composites P_2 and P_3, respectively, for different frequencies. For the composite P_2 the temperature variation curve of σ_{ac} shows that the ac conductivity does not change much up to the frequency 1.2 MHz. For the frequency above 1.2 MHz the ac conductivity first decreases (14–50 K), then increases (50–200 K) with the increase of the temperature and after 200 K slightly decreases. For the composite P_3 similar behavior was found. In the temperature range 50–200 K the ac conductivity increases almost linearly with temperature in consonance with the prediction of the QMT model.

Finally, we have presented the carefully measured experimental observations and it can be concluded that all the aspects of the ac conductivity behavior of the present composite system cannot be reconciled completely with the predictions of any of the above theories. Maybe the over doped composites follow some other theory which needs further investigation.

C. Thermoelectric power

The thermoelectric power is a zero current transport coefficient and is a very useful probe to study the semiconducting and metallic behavior of the composite since it offers a characteristic difference in the two cases. Figure 8 presents the thermal variation of the thermoelectric power of the samples from 77 to 300 K. The four samples exhibit similar nature of the temperature dependence, only the absolute value of the thermopower for different samples differs. The thermoelectric power is positive, low, and varies linearly with temperature. This linear contribution to the thermopower reflects the highly conductive character within the composites and bears a signature of very high intrinsic conductivity. Moreover, because the thermopower is an intrinsic property of the polymer chain, a similar nature of the curves in Fig. 8 indicates that the microscopic chain structures of all the samples studied remain similar. The sign of the thermoelectric power describes the type of majority carriers present in the composite at a certain temperature. The positive sign of thermopower is a signature of the hole conduction and upholds the presence of polarons and/or bipolarons as the cationic charge carriers in our composite samples. It should be recalled that for all the samples studied, polypyrrole content exceeds the percolation threshold and polypyrrole exists in a highly oxidized state in these composites. In this state the empty bipolaronic band overlaps with the p band, giving rise to empty states in the valance band. This will lead to a p

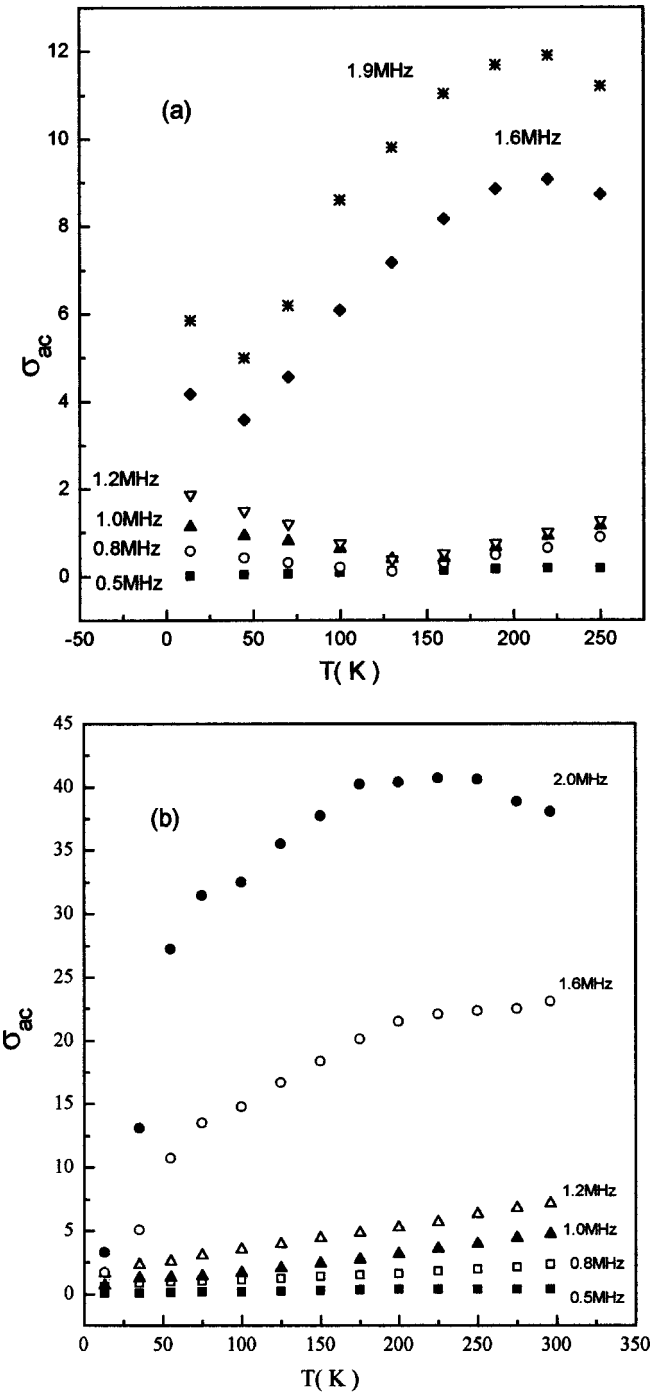

FIG. 7. (a) Thermal variation of the ac conductivity of the composite P_2 obtained by subtracting the dc part of the total conductivity for six different frequencies. (b) The ac conductivity of the composite P_3 plotted as a function of temperature for six particular frequencies.

type metallic conductivity and offers low and positive value of the thermoelectric power as is observed in our case.

Therefore, the temperature dependence of thermopower is consistent with the characteristic diffusion thermopower of a metal and is given by the Mott expression[24]

$$S(T)=(\pi^2/3)(k_B/e)(k_BT)[d\ln\sigma(E)/dT]_{E_F}, \qquad (21)$$

where E_F is the Fermi energy, $\sigma(E)$ is the energy dependent conductivity, k_B is the Boltzman constant, and e is the electronic charge. At high temperatures the downward bending from the linearity manifests that the variable range hopping component is operative in this temperature regime. The overall nature of the curves in Fig. 8 implies that in addition to a contribution from hopping, a linear metal like component is also active for the thermopower and the composites are heterogeneous since the derivation of the Mott formula assumes that the medium is to be homogeneous. Therefore, in these composites we observe that the temperature dependence of conductivity is predominantly nonmetallic and the VRH mechanism plays an important role, but thermopower shows metallic behavior.

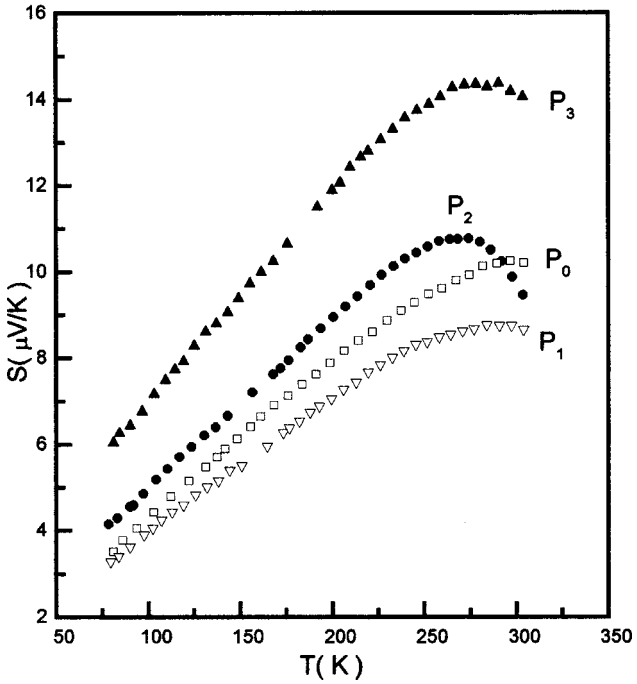

FIG. 8. Variation in thermopower (S) with temperature for the four samples (P_0, P_1, P_2, P_3).

IV. CONCLUSIONS

To conclude we may summarize the results of the electrical transport measurements. In opposition to the present idea that the conductivity of the composites increases with the increase in the conducting component, here the conductivity of the composites increases with the increase of the insulating component. From the analysis by the Mott and Austin formula the parameters obtained are unacceptably low. Therefore at high temperatures the temperature dependence of the dc conductivity does not follow the Mott model of the phonon-assisted polaron hopping mechanism. The dc conductivity data nicely fit with Mott's VRH theory. In the case of ac conductivity, the conductivity increases slowly with frequency up to a characteristic frequency followed by a sudden discontinuous rise and then it begins to increase monotonically with the increase of frequency. In the frequency range from the critical frequency to the maximum investigated frequency, the ac conductivity follows the relation $\sigma = A\omega^{\mathbf{s}}$. The frequency exponent **s** decreases with increasing temperature. This behavior is consistent with the

prediction of the CBH model. The ac conductivity varies almost linearly with temperature in a certain temperature range as predicted by the QMT model of nonoverlapping small polarons. No existing theory can explain all aspects of the temperature and frequency dependence of the ac conductivity. The thermoelectric power varies linearly with temperature like a metal with a downward bending at high temperatures, i.e., in addition to a contribution from hopping a linear metallike part is also active for the thermopower. The heterogeneous model can account for the conflict between the linear metallike behavior of thermopower and semiconductorlike behavior of conductivity. In this model highly conducting metallic islands are interconnected by poorly conducting barriers in a complicated fashion. The metallic regions have a higher thermal resistance and smaller electrical resistance, whereas the barrier regions have a higher electrical resistance and smaller thermal resistance if the barriers are thin. But no single model is found to explain all the details of the ac conductivity behavior.

ACKNOWLEDGMENTS

The authors are grateful to Professor B. G. Ghosh, Professor R. Ranganathan, and Professor K. K. Bardhan of the Low Temperature Physics Division for extending their laboratory facilities. Technical assistance from A. Pal and A. Chakrabarti is also sincerely acknowledged. R. G. acknowledges the CSIR for awarding the Research Fellowship.

[1] H. Q. Xie, Y. M. Ma, and J. S. Guo, Polymer **40**, 261 (1998).
[2] S. G. Han and S. S. Im, J. Appl. Polym. Sci. **67**, 1863 (1998).
[3] F. Selampinar, U. Akbulut, E. Yildiz, A. Gungor, and L. Toppare, Synth. Met. **89**, 111 (1997).
[4] Y. A. Dubitsky, E. A. Becturov, and B. A. Zhubanov, Mater. Chem. Phys. **34**, 306 (1993).
[5] S. P. Armes, S. Gottesfeld, J. G. Beery, F. Garzon, and S. F. Agnew, Polymer **32**, 2325 (1991).
[6] M. Gill, S. P. Armes, D. Fairhurst, S. N. Emmett, G. Idzorek, and T. Pigott, Langmuir **8**, 2178 (1992).
[7] R. Flitton, J. Johal, S. Maeda, and S. P. Armes, J. Colloid Interface Sci. **173**, 135 (1995).
[8] S. Maeda and S. P. Armes, Synth. Met. **69**, 499 (1995).
[9] S. Maeda and S. P. Armes, Chem. Mater. **7**, 171 (1995).
[10] L. M. Gan, L. H. Zhang, H. S. O. Chan, and C. H. Chew, Mater. Chem. Phys. **40**, 94 (1995).
[11] K. Kawai, N. Mihara, S. Kuwabata, and H. Yoneyama, J. Electrochem. Soc. **137**, 1793 (1990).
[12] A. Bhattacharya, K. M. Ganguly, A. De, and S. Sarkar, Mater. Res. Bull. **31**, 527 (1996).
[13] S. T. Selvan, Chem. Commun. (Cambridge) 351 (1998).
[14] S. S. Ray and M. Biswas, Polymer **39**, 6423 (1998).
[15] K. L. N. Phani, S. Pitchumani, and S. Ravichandran, Langmuir **9**, 2455 (1993).
[16] S. Sukeerthi and A. Q. Contractor, Chem. Mater. **10**, 2412 (1998).
[17] R. Gangopadhyay and A. De, Eur. Polym. J. **35**, 1985 (1999).
[18] M. Reghu, C. O. Yoon, C. Yang, D. Moses, A. J. Heeger, and Y. Cao, Macromolecules **26**, 7245 (1993).
[19] V. Jousseaume, M. Morsli, A. Bonnet, D. Tesson, and S. Lefrant, J. Polym. Sci., Polym. Chem. Ed. **67**, 1205 (1998).
[20] E. Benseddik, A. Bonnet, and S. Lefrant, J. Polym. Sci., Polym. Chem. Ed. **68**, 709 (1998).
[21] C. O. Yoon, M. Reghu, D. Moses, A. J. Heeger, and Y. Cao, Synth. Met. **63**, 47 (1994).
[22] R. Singh, R. P. Tandon, and S. Chandra, J. Appl. Phys. **70**, 243 (1991).
[23] N. F. Mott, J. Non-Cryst. Solids **I**, 1 (1968).
[24] N. F. Mott and E. A. Davis, *Electronic Processes in Non-crystalline Materials* (Clarendon, Oxford, 1979).
[25] I. G. Austin and N. F. Mott, Adv. Phys. **18**, 41 (1969).
[26] D. K. Paul and S. S. Mitra, Phys. Rev. Lett. **31**, 1000 (1973).
[27] V. Ambegaokar, B. I. Halprin, and J. S. Langer, Phys. Rev. B **4**, 2612 (1971).
[28] H. Fritzsche, *Amorphous Semiconductors*, edited by J. Tauc (Plenum, New York, 1974), p. 233.
[29] M. H. Brodsky and R. J. Gambino, in *Proceedings of the 4th International Conference on Amorphous and Liquid Semiconductors*, Ann Arbor, MI, 1971, edited by M. H. Cohen and G. Lokovosky (North Holland, Amsterdam, 1972), p. 742.
[30] J. L. Bredas, J. C. Scott, K. Yakushi, and G. B. Street, Phys. Rev. B **30**, 1023 (1984).
[31] R. Singh, R. P. Tandon, and S. Chandra, J. Phys.: Condens. Matter **5**, 1313 (1993).
[32] A. K. Jonscher, Nature (London) **267**, 673 (1977).
[33] A. K. Jonscher, *Dielectric Relaxation in Solids* (Dielectrics, London, Chelsea, 1983).
[34] S. R. Elliot, Adv. Phys. **36**, 135 (1987).
[35] R. Singh, R. P. Tandon, V. S. Panwer, and S. Chandra, J. Appl. Phys. **69**, 2504 (1991).
[36] S. K. Saha, T. K. Mandal, B. M. Mandal, and D. Chakravorty, J. Appl. Phys. **81**, 2646 (1997).
[37] Y. Hirai, H. Tanaka, and T. Nishi, Jpn. J. Appl. Phys., Part 2 **26**, L1401 (1987).
[38] T. H. Ezquerra, F. Kremer, M. Mohammadi, J. Ruhe, G. Wegner, and B. Wessling, Synth. Met. **28**, C83 (1989).
[39] M. Pollak and T. H. Geballe, Phys. Rev. **122**, 1742 (1961).
[40] M. Pollak, Philos. Mag. **23**, 519 (1971).
[41] H. Bottger and V. V. Briskin, Phys. Status Solidi B **78**, 415 (1976).
[42] A. L. Efross, Philos. Mag. B **43**, 829 (1981).
[43] A. R. Long, Adv. Phys. **31**, 553 (1982).
[44] M. Pollak, Phys. Rev. A **138A**, 1822 (1965).
[45] G. E. Pike, Phys. Rev. B **6**, 1572 (1972).
[46] S. R. Elliot, Philos. Mag. **36**, 1291 (1977).
[47] A. Ghosh, Phys. Rev. B **42**, 3663 (1990).
[48] S. Mandal and A. Ghosh, J. Phys.: Condens. Matter **7**, 9543 (1995).